Journal of Interdisciplinary Mathematics
ISSN: 0972-0502 (Print), ISSN: 2169-012X (Online)
Vol. 29 (2026), No. 9, pp. 2653–2671
DOI : 10.47974/JIM-2658

Internal synchronization and anti-synchronization using active control

Mohammed Raziuddin *
Mohammed Naheed †
Mohammad Shahzad §
Department of Supportive Requirements-Sciences and Mathematics
University of Technology and Applied Sciences
Nizwa 611
Sultanate of Oman

Abstract

In this study, the theme of internal synchronization and anti-synchronization is proposed as the coordination between combinations (subsystems) of a universal chaotic/hyper-chaotic dynamical system. The study demonstrates the versatility of the approach by constructing switches of different heterogeneous orders, thereby extending its applicability. Three distinct types of heterogeneous switches during internal multi-switching synchronization and anti-synchronization are formulated using active control strategies. To validate the proposed framework, a Seven-Dimensional Hyper Chaotic System (7DHCS), characterized by twelve positive constraints and seven nonlinear terms, is selected as a representative case study. An extensive computational study is performed to verify the accuracy of the analytical solutions, ensuring the robustness and Lyapunov stability.

Subject Classification: *93D05, 34H10, 93C10.*

Keywords: *Internal synchronization, Internal anti-synchronization, Active control, Hyperchaotic system, Lyapunov exponent, Gain constant.*

1. Introduction

The potential applications and development opportunities of chaos control and synchronization across various fields, including biological sciences, engineering, and sociological models, and other sciences, have garnered significant research attention [1-2]. The chaos synchronization together with improved method has continuously received considerable attention due to its practical simplicity [3–5]. Since last three decades, researchers have made notable contributions to chaos synchronization using fuzzy control, sliding

* *E-mail:* **mohammed.raziuddin@utas.edu.om (Corresponding Author)**
† *E-mail:* **naheed.mohammed@utas.edu.om**
§ *E-mail:* **mohammed.shehzad@utas.edu.om**

© Taru Publications

mode, active control etc. successfully synchronizing nonlinear systems [6-9]. However, chaos synchronization has typically been limited to synchronizing two identical/non-identical chaotic systems with various kind of synchronization techniques. Multi-switching synchronization refers to the phenomenon where multiple dynamical systems synchronize in a coordinated manner despite switching between different states or modes. Through the application of active control method, Ucar, Lonngren, and Bai [10] studied the multi-switching synchronization of coupled chaotic systems and demonstrated successful synchronization in the Lorenz system. The multi-synchronization of Lorenz & Chen systems with uncertain parameters was studied by Wang and Sun [11]. Using Lyapunov theory on stability, they formulated controllers and updating laws tailored to different switch combinations.

Over the last decade, this phenomenon has been extensively studied and has many applications in various fields, including communication systems, power systems and control engineering, etc. [12-17]. There have been several studies on multi-switching synchronization, and these studies have explored different aspects of the phenomenon.

Overall, the literature on multi- switching synchronization is extensive and covers various aspects of this phenomenon. The studies have explored the synchronization of chaotic systems, networked systems, power systems and multi-agent systems, among others. These studies have demonstrated the potential of multi-switching synchronization in various applications and have provided insights into the mechanisms behind this phenomenon [18-24]. Recently, Martinez, Gomez, and Espina [25] explored multi-switching compound synchronization using optimal control for four non identical chaotic systems. They proposed a technique based on linearizing the slave system using the Jacobian matrix. Khan, Khattar, and Agrawal [26] presented a new approach of anti-difference multi-switching compound-compound combination synchronization taking seven chaotic systems. In this approach, it has been taken five drive and two response systems. Furthermore, in order to achieve the synchronization, Lyapunov stability criteria has been used. Liu, Li, and He [27] studied the fixed time multi-switching combination-combination synchronization of fractional order chaotic systems under the effects of uncertainties and external disturbances. The fixed time multi-switching combination-combination synchronization using sliding mode control is done between four fractional chaotic systems. Motivated by the above mentioned studies, the authors plan to study the IMSS and IMSAS for a universal chaotic system using active control. For the demonstration purposes, a 7DHCS has been chosen as a universal chaotic system. The idea behind choosing active control is that it is one of the most widely used technique for the kind of synchronizations under study for the chaotic systems. It included many features like mitigating unwanted disturbances, enhancing system performance and providing robust stability [5].

The main highlights of our study are as follows:

- Designing heterogeneous combinations through different orders of leader's and follower's subsystems from a universal chaotic/hyper chaotic system.
- Testing the heterogeneous combinations for both IMSS and IMSAS cases.
- Verifying the analytical results for through computational study using Mathematica.

The continuation of this work is presented in the following manner: In section 2, problem statement has been described. In section 3, designing of heterogeneous combinations for 7DHCS have been discussed and lastly concluding remarks are there in section 4.

2. Problem Statement

IMSS and IMSAS involve synchronizing different subsets of a single chaotic/hyper-chaotic system's state variables with each other. This can be achieved using different types of combinations depending on the error. By synchronizing specific subsets of the state vectors internally, internal synchronization can reveal important insights into the system's underlying dynamics.

Let us consider a chaotic/hyperchaotic system below

$$\dot{\boldsymbol{x}}(t) = \boldsymbol{A}\boldsymbol{x} + \boldsymbol{f}(\boldsymbol{x}) \tag{1}$$

Where, $\boldsymbol{x} = [x_1, x_2, x_3, ..., x_n]^T \in R^n$ are the state vector, $A \in R^m$ represents the unknown constant parameters vector of the system, $\boldsymbol{f}(\boldsymbol{x})$ is an $n \times 1$ matrix of nonlinear continuous functions.

Now break the system into two subsystems,

Leader subsystem: $\dot{x_1}(t) = A_1 x_1 + f_1(x)$ (2)

Follower subsystem: $\dot{x_2}(t) = A_2 x_2 + f_2(x)$ (3)

where $\boldsymbol{x_1}, \boldsymbol{x_2} \subset \boldsymbol{x}$ and $\boldsymbol{x_1}$ and $\boldsymbol{x_2}$ are disjoints and $\boldsymbol{u}(t) \in R^{n_1}$ represents a controlling matrix, $x_1, x_2 \in R^{n_1}$ are the state vector, $f_1(x)$ and $f_2(x)$ are the $n_1 \times l$ matrices of nonlinear continuous functions.

The IMSS and IMSAS problem is reformulated as stabilizing the error dynamics of leader–follower subsystems with unknown parameters. To achieve this, a tailored control law $u(t)$ is designed, ensuring the stability of the error subsystems.

i.e. $\lim_{t\to\infty} \|x_j(t) \pm x_i(t)\| \to 0$ for $x_i \in x_1$ and $x_j \in x_2$.

Theorem 1: *Let the control function is* $\dot{e}(t) = ke(t) + L(x_1, x_2, t) + u(t)$

The IMSS and IMSAS problem can be reformulated as the equivalent task of stabilizing the error system derived from the leader-follower sub-systems, governed by the unknown parameters. This transformation provides a novel framework for addressing stability challenges in complex chaotic subsystems.

$$u(t) = -L_1(x_1, x_2, t) + v(t) \tag{4}$$

Where the linear controller vector $v(t)$, *is defined as* $v(t) = -we(t)$ (5)

Where $w \in R^{n_1 \times n_1}$ *is a feedback constant gain diagonal matrix.*

Proof: The error dynamics of (2) and (3) is given by

$$\dot{e}(t) = ke(t) + L(x_1, x_2, t) + u(t) \tag{6}$$

$$\dot{e}(t) = (k - w)e(t) \tag{7}$$

As per the Ruth-Hurwitz criterion, the two chaotic subsystems will synchronized global asymptotically if and only if $(k - w)$is a Hurwitz matrix [28]. Suppose a Positive Definite Lyapunov Function (PDLF) is established to facilitate stability investigation.

$$V(t) = \frac{1}{2} e^t M e \tag{8}$$

3. IMSS in 7DHCS

For illustration purposes, we have chosen 7DHCS [29]. In the selected system, three types of combinations are identified, namely those based on single, double, and triple errors.

$$\text{7DHCS}=\begin{cases} \dot{x_1} = -\sigma x_1 + \rho x_2 + \delta x_3 - \eta x_4 \\ \dot{x_2} = \Omega x_1 - \psi x_1 x_3 - \mu x_2 \\ \dot{x_3} = -\phi x_3 + x_1 x_2 + \eta x_4 \\ \dot{x_4} = x_2 x_7 + \beta x_1 x_7 - \eta x_3 - x_4 \\ \dot{x_5} = -x_5 - \mho x_2 x_3 - \phi x_4 x_7 \\ \dot{x_6} = -\omega x_6 - \mu x_3 x_5 x_7 + \Omega x_1 x_7 \\ \dot{x_7} = -\alpha x_7 + x_1 x_2 + \eta x_4 \end{cases} \tag{9}$$

Where x_i (for $i = 1$ to 7) are the state vectors; $\sigma, \rho, \delta, \eta, \Omega, \psi, \mho, \phi, \beta, \omega, \mu.$ and α are the parameters from the above system. During simulation, we have taken their values as $\sigma = 14, \rho = 11, \delta = 0.4, \eta = 0.5, \Omega = 30, \psi = 2.5, \mho = 3, \phi = 5, \beta = 2, \omega = 15, \mu = 4, \alpha = 13$ and the initial conditions $x_1 = 0.1, x_2 = 0.5, x_3 = 3.5, x_4 = 0.1, x_5 = 0.6, x_7 = 0.6$ for simulation. In the present study, both IMSS and IMSAS are represented through the 7DHCS, which exhibits three types of internal synchronization characteristics, namely three distinct combinations as outlined below.

1. Single error based combinations:

$$\underbrace{\begin{bmatrix} S_1 \\ S_2 \\ . \\ . \\ . \\ S_{30} \end{bmatrix} \rightarrow \begin{bmatrix} e_{1,1} \\ e_{2,1} \\ . \\ . \\ . \\ e_{30,1} \end{bmatrix} = \begin{bmatrix} x_1 \pm x_2 \\ x_1 \pm x_3 \\ . \\ . \\ . \\ x_3 \pm x_4 \end{bmatrix}}_{\text{Combinations having single error}} \tag{10}$$

2. Double errors based combinations:

$$\underbrace{\begin{bmatrix} S_1 \\ S_2 \\ . \\ . \\ . \\ S_{90} \end{bmatrix} \rightarrow \begin{bmatrix} e_{1,1} & e_{1,2} \\ e_{2,1} & e_{2,2} \\ . & . \\ . & . \\ . & . \\ e_{90,1} & e_{90,2} \end{bmatrix} = \begin{bmatrix} x_1 \pm x_3 & x_2 \pm x_4 \\ x_1 \pm x_4 & x_2 \pm x_3 \\ . & . \\ . & . \\ . & . \\ x_3 \pm x_1 & x_4 \pm x_2 \end{bmatrix}}_{\text{Combinations having two errors}} \tag{11}$$

3. Triple errors based combinations:

$$\underbrace{\begin{bmatrix} S_1 \\ S_2 \\ . \\ . \\ . \\ S_{20} \end{bmatrix} \rightarrow \begin{bmatrix} e_{1,1} & e_{1,2} & e_{1,3} \\ e_{2,1} & e_{2,2} & e_{2,3} \\ . & . & . \\ . & . & . \\ . & . & . \\ e_{20,1} & e_{20,2} & e_{20,3} \end{bmatrix} = \begin{bmatrix} x_4 \pm x_1 & x_5 \pm x_2 & x_6 \pm x_3 \\ x_3 \pm x_1 & x_5 \pm x_2 & x_6 \pm x_4 \\ . & . & . \\ . & . & . \\ . & . & . \\ x_3 \pm x_1 & x_4 \pm x_2 & x_4 \pm x_2 \end{bmatrix}}_{\text{Combinations having three errors}} \tag{12}$$

Note: In this error '$\pm$' is for anti-synchronization and synchronization respectively.

3.1 *IMSS based on single error*

This section examines the IMSS and IMSAS between the subsystems based on the state variable from the 7DHCS (9). We limit our discussion to three homogeneous combinations, as the remaining cases follow the same logic. We conduct a parallel analytical study for both cases (i.e. synchronization and anti-synchronization).

Combination 1: We propose designing two subsystems derived from equation (9) to capture the dynamics of x_1 and x_5 for the purpose of synchronization as well as anti-synchronization, as follows

$$\text{Leader subsystem} : \dot{x_1} = -\sigma x_1 + \rho x_2 + \delta x_3 - \eta x_4,$$
$$\text{Follower subsystem} : \dot{x_5} = -x_5 - \mho x_2 x_3 - \phi x_4 x_7 + u_{1,1} \tag{13}$$

Deriving from (10) and (13), the error dynamics governing combination-1 can be formulated as:

$$\dot{e}_{1,1} = -(1+\sigma)e_{1,1} + u_{1,1} \tag{14}$$

Where $u_{1,1} = \dot{x}_1 - \sigma\dot{x}_5 + \mho x_2 x_3 + \phi x_4 x_7 + \rho x_2 + \delta x_5 - \eta x_4 + v_{1,1}$ (15)

Now, from (14) and (15), we have

$$\dot{e_{1,1}} = -(1+\sigma+k_{11})e_{1,1} \tag{16}$$

Where $v_{1,1} = -k_{11}e_{1,1}$

For the purpose of stability analysis, let us introduce a PDLF

$$V_{1,1}(t) = \frac{1}{2}{e_{1,1}}^2 \tag{17}$$

$$\dot{V}_{1,1} = -(1 + \sigma + k_{11}){e_{1,1}}^2 \quad \text{for } \dot{V}_{1,1}(t) < 0 \tag{18}$$

$$k_{11} > -(1 + \sigma).$$

Similarly, it can be computed for anti-synchronization case

$$\dot{V}_{1,1} = -(1 + \sigma + k_{11}){e_{1,1}}^2 \tag{19}$$

For $V_{1,1}(t) < 0 \Longrightarrow \quad k_{11} > -(1 + \sigma)$.

Combination 2: We propose designing two subsystems derived from equation (9) to capture the dynamics of x_2 and x_4 for the purpose of synchronization as well as anti-synchronization, as follows

Leader subsystem: $\dot{x_2} = \Omega x_1 - \psi\rho x_1 x_3 - \mu x_2$,

Follower subsystem: $\dot{x_4} = x_2 x_7 + \beta x_1 x_7 - \eta x_3 - x_4 + u_{21}$. (20)

Deriving from (10) and (20), the error dynamics governing combination-2 can be formulated as:

$$\dot{e_{2,1}} = -(1 + \mu)e_{2,1} + u_{2,1} \tag{21}$$

Where

$$u_{2,1} = x_2 - \mu x_2 - x_2 x_7 - \beta x_1 x_7 + \eta x_3 + \Omega x_1 - \psi x_1 x_3 + v_{2,1} \tag{22}$$

Now, from (21) and (22), we have

$$\dot{e_{2,1}} = -(1 + \mu + k_{21})e_{2,1} \text{ , where } v_{2,1} = -k_{21}e_{2,1} \tag{23}$$

For the purpose of stability analysis, let us introduce a PDLF

$$V_{2,1}(t) = -\frac{1}{2}e_{2,1}^2 \tag{24}$$

$$\dot{V}_{2,1} = -(1 + \mu + k_{21})e_{2,1}^2 \tag{25}$$

For $\dot{V}_{2,1} < 0 \implies k_{21} > -(1 + \mu)$

Similarly, it can be computed for anti-synchronization case

$$\dot{V}_{2,1} = -(1 + \mu + k_{21})e_{2,1}^2 \tag{26}$$

For $\dot{V}_{2,1} < 0 \implies k_{21} > -(1 + \mu)$

Combination 3: We propose designing two subsystems derived from equation (9) to capture the dynamics of x_3 and x_6 for the purpose of synchronization as well as anti-synchronization, as follows

Leader subsystem: $\dot{x_3} = -\phi x_3 + x_1 x_2 + \eta x_4$

Follower subsystem: $\dot{x_6} = -\omega x_6 - \mu x_3 x_5 x_7 + \Omega x_1 x_7 + u_{31}$ (27)

Deriving from (10) and (27), the error dynamics governing combination-3 can be formulated as:

$$\dot{e_{3,1}} = -(\omega + \phi)e_{3,1} \tag{28}$$

Where $u_{3,1} = \omega x_3 - \phi x_6 + \mu x_3 x_5 x_7 - \Omega x_1 x_7 + x_1 x_2 + \eta x_4 + v_{3,1}$ (29)

Now, from (25) and (26), we have

$$\dot{e_{3,1}} = -(\omega + \phi + k_{31})e_{3,1} \text{ , where } v_{3,1} = -k_{31}e_{3,1} \tag{30}$$

For the purpose of stability analysis, let us introduce a PDLF

$$V_{3,1}(t) = \frac{1}{2}e_{3,1}^2 \tag{31}$$

$$\dot{V}_{3,1}(t) = -(\omega + \phi + k_{31})e_{3,1}^2, \tag{32}$$

For $\dot{V}_{3,1}(t) < 0 \implies k_{31} > -(\omega + \phi)$,

Similarly, it can be computed for anti-synchronization case

$$\dot{V}_{3,1}(t) = -(\omega + \phi + k_{31})e_{3,1}^2 , \tag{33}$$

For $\dot{V}_{3,1}(t) < 0 \implies k_{31} > -(\omega + \phi)$,

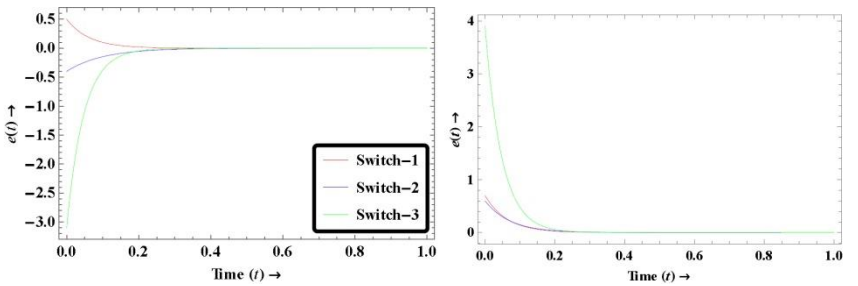


Figure 1

Time series graph of errors for the first order of selected three combinations during (a) synchronization (b) anti-synchronization.

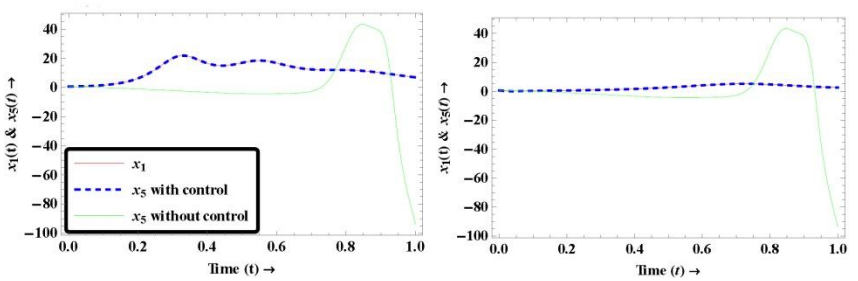


Figure 2

Time series analysis of $x_1(t)$ and $x_5(t)$ (controlled & uncontrolled both) for the first combination of first order (a) synchronization (b) anti-synchronization.

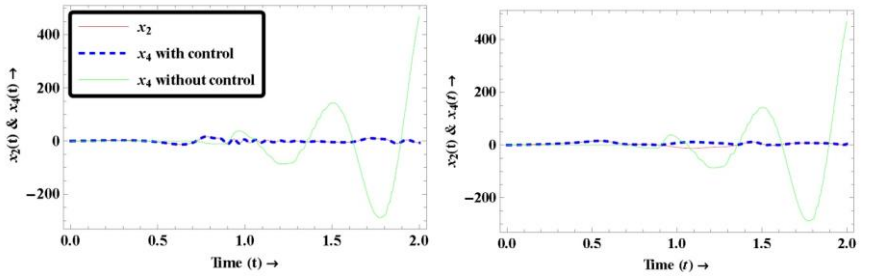


Figure 3

Time series graph of $x_2(t)$ and $x_4(t)$ (controlled & uncontrolled both) for the second combination of first order (a) synchronization (b) anti-synchronization.

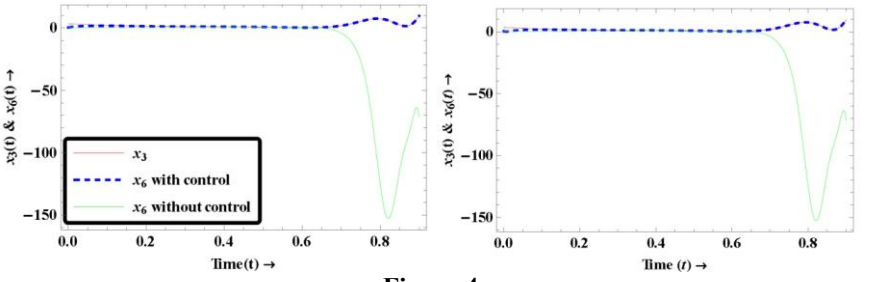


Figure 4

Time series analysis of $x_3(t)$ and $x_6(t)$ (controlled & uncontrolled both) for the third combination of first order (a) synchronization (b) anti-synchronization.

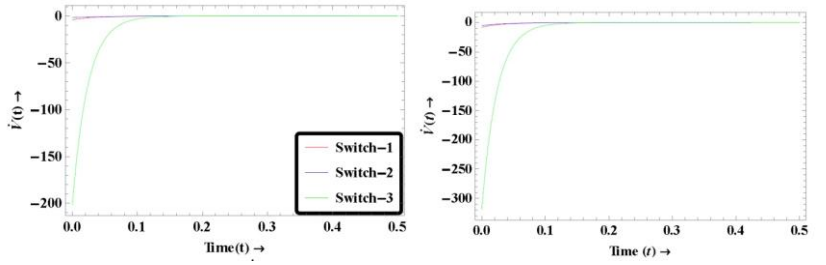


Figure 5

Time series analysis of $\dot{V}(t)$ for the three selected combinations of first order (a) synchronization (b) anti-synchronization.

In this subsection, IMSS and IMSAS have been presented for the combinations that have single error. We have discussed only three combinations out of 30 combinations (see equation (10)), the remaining combinations can be studied analogously and therefore are omitted here for brevity. In the proposed study, for the simulation of three combinations, the gain constants for the presented combinations are chosen $k_{11} = 1$, $k_{21} = 0.21$, $k_{31} = 1$ for

simulation on Mathematica for both synchronization and anti-synchronization. A parallel analytical and computational studies are carried out for both synchronization and anti-synchronization cases. Also, all Figures are divided into two parts (a) and (b) where (a) is for synchronization and (b) is for anti-synchronization. Figures 1–4 provide a comprehensive visualization of the error dynamics with respect to time (t) alongside the state variables (controlled & uncontrolled). Figures 1–5 collectively demonstrate that the combinations evaluated met the predefined satisfaction criteria for the asymptotic stability during synchronization and anti-synchronization. Furthermore, the derivative of Lyapunov function with respect to t, confirm the asymptotic stability for both the cases in Figure 5, demonstrating unambiguously that all combinations achieved the required level of stability. However, a significant difference is not there between synchronization and anti-synchronization. But during synchronization a minute delay can be seen in the time response of synchronization for all three first order of combinations under study (see Figure 1 (a) and (b)).

3.2 *IMSS based on two errors*

The subsection explores the IMSS and IMSAS of two subsystems, each with two state variables from 7DHCS. The authors study the first two combinations, triggered by two error signals, and suggest a similar approach for the remaining combinations. The subsection also provides a parallel analytical investigation of both synchronization and anti-synchronization cases.

Combination 1: In the combination-1 of order two, we propose designing two subsystems derived from equation (9) to capture the dynamics of $x_1 \,\&\, x_2$ and $x_5 \,\&\, x_4$ for the purpose of synchronization as well as anti-synchronization, considering the two state variables derived from (9), with $e_{1,1} = x_5 \pm x_1$ and $e_{1,2} = x_4 \pm x_2$ specified as follows

$$\text{Leader Subsystem:} \quad \begin{bmatrix} \dot{x}_1 \\ \dot{x}_2 \end{bmatrix} = \begin{bmatrix} -\sigma x_1 + \rho x_2 + \delta x_5 - \eta x_4 \\ \Omega x_1 - \psi x_1 x_3 - \mu x_2 \end{bmatrix},$$

$$\text{Follower Subsystem:} \begin{bmatrix} \dot{x}_5 \\ \dot{x}_4 \end{bmatrix} = \begin{bmatrix} -x_5 - \mho x_2 x_3 - \phi x_4 x_7 \\ x_2 x_7 + \beta x_1 x_7 - \eta x_3 - x_4 \end{bmatrix} + \begin{bmatrix} u_{1,1} \\ u_{1,2} \end{bmatrix} \tag{34}$$

Deriving from (11) and (33), the error dynamics governing combination-1 can be formulated as:

$$\begin{aligned} \dot{e}_{1,1} &= -(1+\sigma)e_{1,1} + u_{1,1} \\ \dot{e}_{1,2} &= -(1+\mu)e_{1,2} + u_{1,2} \end{aligned} \tag{35}$$

Where

$$\begin{aligned} u_{1,1} &= x_1 - \sigma x_5 + \mho x_2 x_3 + \phi x_4 x_7 + \rho x_2 + \delta x_5 - \eta x_4 + v_{1,1} \\ u_{1,2} &= x_2 - \mu x_4 - x_2 x_7 - \beta x_1 x_7 + \eta x_3 + \Omega x_1 - \psi x_1 x_3 + v_{1,2} \end{aligned} \tag{36}$$

Accordingly, equation (34) may be rewritten as

$$\dot{e_{1,1}} = -(1+\sigma+k_{11})e_{1,1} + v_{1,1} \quad \text{where } v_{1,1} = -k_{11}e_{1,1}$$
$$\dot{e_{1,2}} = -(1+\mu+k_{12})e_{1,2} + v_{1,2} \quad \text{and } v_{1,2} = -k_{12}e_{1,2} \tag{37}$$

For the purpose of stability analysis, let us introduce a PDLF

$$V_{1,1}(t) = \frac{1}{2}(e_{1,1}^2 + e_{1,2}^2) \tag{38}$$

$$\dot{V}_{1,1}(t) = -(1+\sigma+k_{11})e_{1,1}^2 - (1+\mu+k_{12})e_{1,2}^2 \tag{39}$$

For $\dot{V}_{1,1}(t) < 0 \implies k_{11} > -(1+\sigma)$ and $k_{12} > -(1+\mu)$

Similarly, it can be computed for anti-synchronization case

Case: $$\dot{V}_{1,1}(t) = -(1+\sigma+k_{11})e_{1,1}^2 - (1+\mu+k_{12})e_{1,2}^2 \tag{40}$$

For $\dot{V}_{1,1}(t) < 0 \implies k_{11} > -(1+\sigma)$ and $k_{12} > -(1+\mu)$

Combination 2: In the combination-2 of order two, we propose designing two subsystems derived from equation (9) to capture the dynamics of x_2 & x_3 and x_4 & x_6 for the purpose of synchronization as well as anti-synchronization, considering the two state variables derived from (9), with $e_{2,1} = x_4 \pm x_2$ and $e_{2,2} = x_6 \pm x_3$ specified as follows

Leader Subsystem: $$\begin{bmatrix}\dot{x}_2\\ \dot{x}_3\end{bmatrix} = \begin{bmatrix}\Omega x_1 - \psi x_1 x_3 - \mu x_2\\ -\phi x_3 + x_1 x_2 + \eta x_4\end{bmatrix},$$

Follower Subsystem: $$\begin{bmatrix}\dot{x}_4\\ \dot{x}_6\end{bmatrix} = \begin{bmatrix}x_2 x_7 + \beta x_1 x_7 - \eta x_3 - x_4\\ -\omega x_6 - \mu x_3 x_5 x_7 + \Omega x_1 x_7\end{bmatrix} + \begin{bmatrix}u_{2,1}\\ u_{2,2}\end{bmatrix} \tag{41}$$

Deriving from (11) and (40), the error dynamics governing combination-2 can be formulated as:

$$\dot{e_{2,1}} = -(1+\mu)e_{1,2} + u_{2,1}$$
$$\dot{e_{2,2}} = -(\omega+\phi)e_{2,2} + u_{2,2} \tag{42}$$

Where

$$u_{2,1} = x_2 - \mu x_4 - x_2 x_7 - \beta x_1 x_7 + \eta x_3 + \Omega x_1 - \psi\rho x_1 x_3 + v_{2,1},$$
$$u_{2,2} = -\omega x_3 - \phi x_6 + \mu x_3 x_5 x_7 - \Omega x_1 x_7 + x_1 x_2 + \eta x_4 + v_{2,2}, \tag{43}$$

Accordingly, equation (42) may be rewritten as

$$\dot{e_{2,1}} = -(1+\mu+k_{21})e_{1,2},$$
$$\dot{e_{2,2}} = -(\omega+\phi+k_{22})e_{2,2}, \tag{44}$$

Where $v_{2,1} = -k_{21}e_{2,1}$ and $v_{2,2} = -k_{22}e_{2,2}$

For the purpose of stability analysis, let us introduce a PDLF

$$V_{2,1}(t) = \frac{1}{2}(e_{2,1}^2 + e_{2,2}^2) \tag{45}$$

$$\dot{V}_{2,1}(t) = -(1+\mu+k_{21})e_{2,1}^2 - (\omega+\phi+k_{22})e_{2,2}^2 \tag{46}$$

For $\dot{V}_{2,1}(t) < 0 \implies k_{21} > -(1+\mu)$ and $k_{22} > -(\omega+\phi)$

Similarly, it can be computed for anti-synchronization case

Case: $$\dot{V}_{2,1}(t) = -(1+\mu+k_{21})e_{2,1}^2 - (\omega+\phi+k_{22})e_{2,2}^2 \tag{47}$$

For $\dot{V}_{2,1}(t) < 0 \implies k_{21} > -(1+\mu)$ and $k_{22} > -(\omega+\phi)$

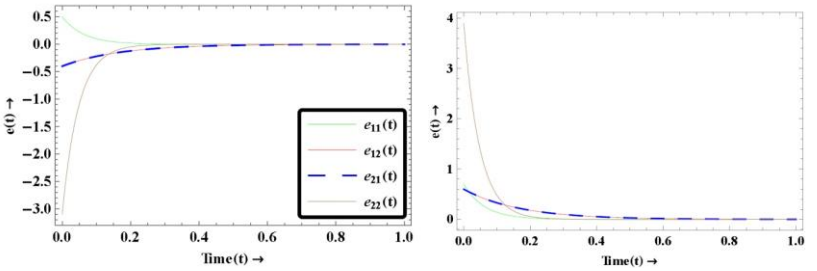


Figure 6

Time series graph of errors for the second order of selected two combinations (a) in synchronization case (b) in anti-synchronization case.

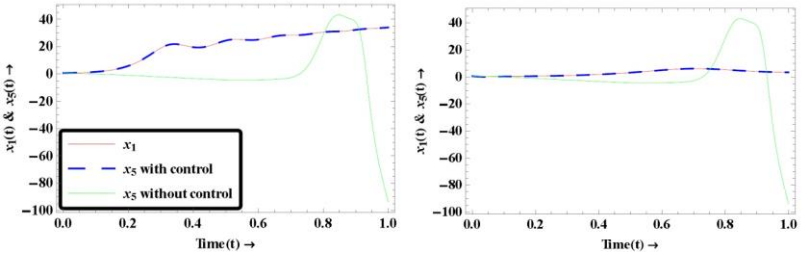


Figure 7

Time series graph of $x_1(t)$ and $x_5(t)$ (controlled & uncontrolled both) for the first combination of second order (a) in synchronization case (b) in anti-synchronization case.

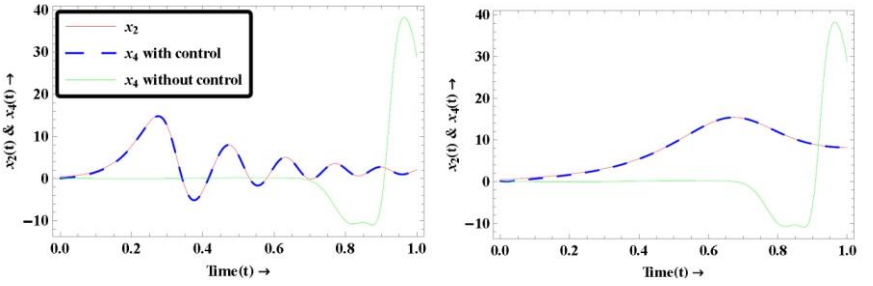


Figure 8

Time series graph of $x_2(t)$ and $x_4(t)$ (controlled & uncontrolled both) for the first combination of second order (a) in synchronization case (b) in anti-synchronization case.

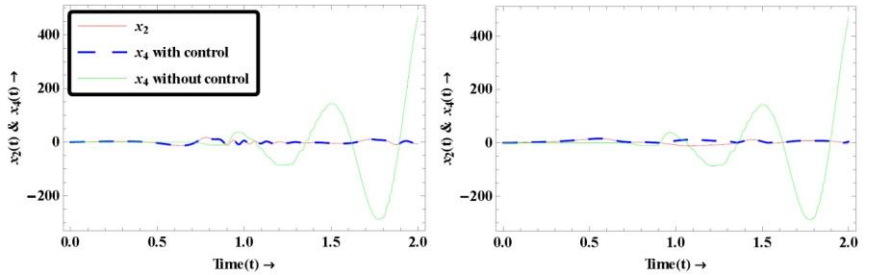


Figure 9

Time series graph of $x_2(t)$ and $x_4(t)$ (controlled & uncontrolled both) for the second combination of the second order (a) in synchronization case (b) in anti-synchronization case.

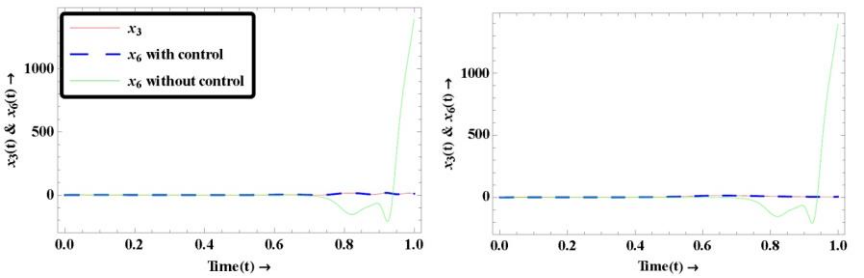


Figure 10

Time series graph of $x_3(t)$ and $x_6(t)$ (controlled & uncontrolled both) for the second combination of the second order (a) in synchronization case (b) in anti-synchronization case.

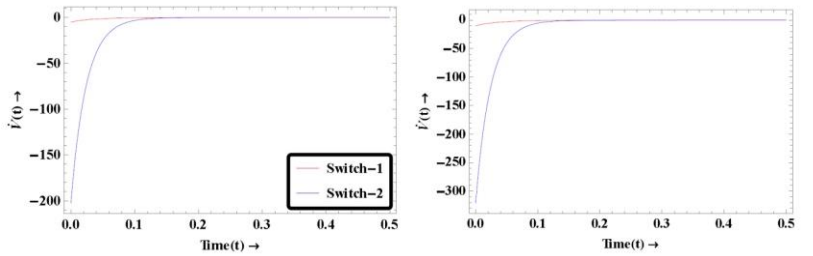


Figure 11

Time series graph of $\dot{V}(t)$ for the two selected combinations of second order (a) in synchronization case (b) in anti-synchronization case.

In this subsection, the IMSS and IMSAS are formulated for the 7DHCS based on two error signals considered across all possible Leader-Follower pairings. Each subsystem in the configuration consists of two state variables. Although a total of 90 such combinations exist (see Equation (11)), only two representative cases are discussed here; the remaining combinations can be

analyzed in an analogous manner. For the simulation of two selected combinations, the illustrative constants $k_{11} = 1, k_{12} = 1, k_{21} = 1, k_{22} = 1$ were used in Mathematica-based computations. A parallel computational assessment was also conducted for both synchronization & anti-synchronization scenarios. The dynamical behavior of the 7DHCS and their corresponding state vectors for the combinations under study are plotted to demonstrate the effectiveness of IMSS and IMSAS (see Figures 6–10). From these Figures, it is evident that both IMSS & IMSAS exhibit robust performance. Moreover, the time-series profile of $\dot{V}(t)$ (Figure 11) clearly indicates that the combinations investigated achieve stability in both cases considered. However, there is not a significant difference can be seen between synchronization and anti-synchronization. But a minute delay can be seen between the time response in both the cases. The combinations of order two are synchronizing slower than the synchronization in the combinations in order one.

3.3 *IMSS based on three errors*

In this section, the analysis of IMSS & IMSAS is presented for two subsystems of the 7DHCS comprising a total of three state variables. Only one representative combination, derived from the three associated error signals, are discussed here; the remaining combinations can be investigated in an analogous manner. A parallel study is carried out for both synchronization and anti-synchronization cases.

Combination 1: In the combination-1 of order three, we propose designing two subsystems derived from equation (9) to capture the dynamics of x_1, x_2 & x_3 and x_4, x_5 & x_6 for the purpose of synchronization as well as anti-synchronization, considering the three state variables derived from (9), with $e_{1,1} = x_5 \pm x_1$, $e_{1,2} = x_4 \pm x_2$ and $e_{1,3} = x_6 \pm x_3$ specified as follows

$$\text{Leader Subsystem: } \begin{bmatrix}\dot{x}_1\\ \dot{x}_2\\ \dot{x}_3\end{bmatrix} = \begin{bmatrix}-\sigma x_1 + \rho x_2 + \delta x_5 - \eta x_4\\ \Omega x_1 - \psi x_1 x_3 - \mu x_2\\ -\phi x_3 + x_1 x_2 + \eta x_4\end{bmatrix},$$

$$\text{Follower Subsystem: } \begin{bmatrix}\dot{x}_4\\ \dot{x}_5\\ \dot{x}_6\end{bmatrix} = \begin{bmatrix}x_2 x_7 + \beta x_1 x_7 - \eta x_3 - x_4\\ -x_5 - \mho x_2 x_3 - \phi x_4 x_7\\ -\omega x_6 - \mu x_3 x_5 x_7 + \Omega x_1 x_7\end{bmatrix} + \begin{bmatrix}u_{1,1}\\ u_{1,2}\\ u_{1,3}\end{bmatrix}. \tag{48}$$

Deriving from (12) and (47), the error dynamics governing combination-1 can be formulated as:

$$\begin{aligned} \dot{e_{1,1}} &= -(1+\sigma)e_{1,1} + u_{1,1},\\ \dot{e_{2,1}} &= -(1+\mu)e_{1,2} + u_{1,2},\\ \dot{e_{1,3}} &= -(\omega+\phi)e_{1,3} + u_{1,3}. \end{aligned} \tag{49}$$

Where

$$u_{1,1} = x_1 - \sigma x_5 + \mho x_2 x_3 + \phi x_2 x_3 + \rho x_2 + \delta x_5 - \eta x_4 + v_{1,1},$$

$$u_{1,2} = x_2 - \mu x_4 - x_2 x_7 - \beta x_1 x_7 + \eta x_3 + \Omega x_1 - \psi x_1 x_3 + v_{1,2},$$

$$u_{1,3} = \omega x_3 - \phi x_6 + \mu x_3 x_5 \rho + \Omega x_1 x_7 - \Omega x_1 \rho + x_1 x_2 + \eta x_4 + v_{1,3}. \quad (50)$$

Now, (43) can be written as

$$\begin{aligned} \dot{e_{1,1}} &= -(1 + \sigma + k_{11}) e_{1,1}, \\ \dot{e_{1,2}} &= -(1 + \mu + k_{12}) e_{1,2}, \\ \dot{e_{1,3}} &= -(\omega + \phi + k_{13}) e_{1,3}. \end{aligned} \quad (51)$$

Where $v_{1,1} = -k_{11} e_{1,1}$, $v_{1,2} = -k_{12} e_{1,2}$ and $v_{1,3} = -k_{13} e_{1,3}$.

For the purpose of stability analysis, let us introduce a PDLF

$$V_{1,1} = \frac{1}{2}(e_{1,1}^2 + e_{1,2}^2 + e_{1,3}^2) \quad (52)$$

$$\dot{V}_{1,1} = -(1 + \sigma + k_{11}) e_{1,1}^2 - (1 + \mu + k_{12}) e_{2,2}^2 - (\omega + \phi + k_{13}) e_{1,3}^2 \quad (53)$$

For $\dot{V}_{1,1}(t) < 0 \implies k_{11} > -(1 + \sigma)$, $k_{12} > -(1 + \mu)$, $k_{13} > -(\omega + \phi)$

Similarly, it can be computed for anti-synchronization case

$$\dot{V}_{1,3} = -(1 + \sigma + k_{11}) e_{1,1}^2 - (1 + \mu + k_{12}) e_{2,2}^2 - (\omega + \phi + k_{13}) e_{1,3}^2 \quad (54)$$

For $\dot{V}_{1,3}(t) < 0 \implies k_{11} > -(1 + \sigma)$, $k_{12} > -(1 + \mu)$, $k_{13} > -(\omega + \phi)$

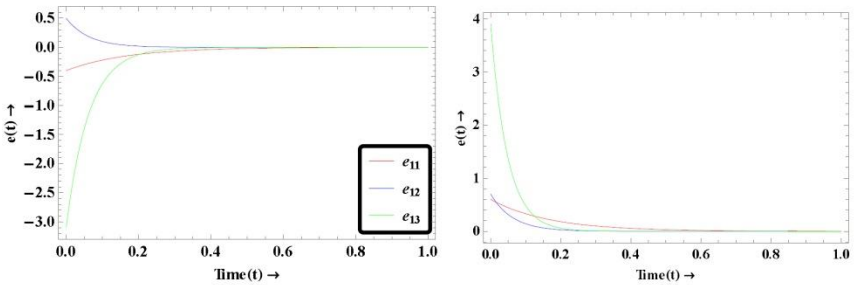


Figure 12

Time series graph of errors for the third order of the selected combination (a) in synchronization case (b) in anti-synchronization case.

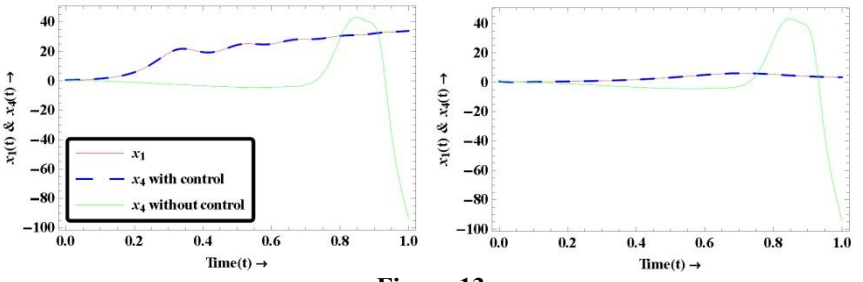


Figure 13

Time series graph of $x_1(t)$ and $x_4(t)$ (controlled & uncontrolled both) for the first combination of the third order (a) in synchronization case (b) in anti-synchronization case.

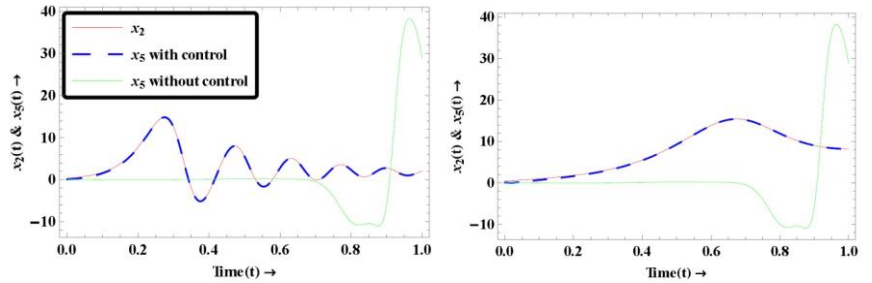


Figure 14

Time series graph of $x_2(t)$ and $x_5(t)$ (controlled & uncontrolled both) for the first combination of the third order (a) in synchronization case (b) in anti-synchronization case.

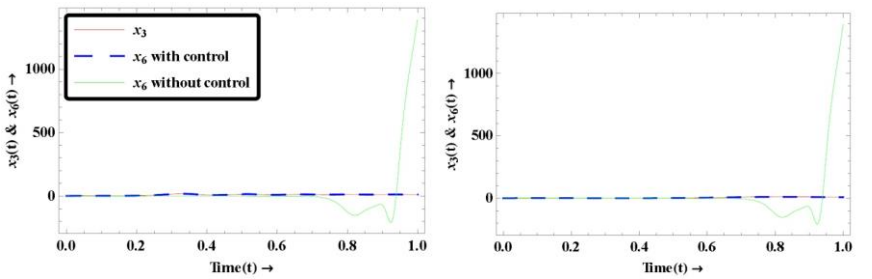


Figure 15

Time series graph of $x_3(t)$ and $x_6(t)$ (controlled & uncontrolled both) for the first combination of third order (a) in synchronization case (b) in anti-synchronization case.

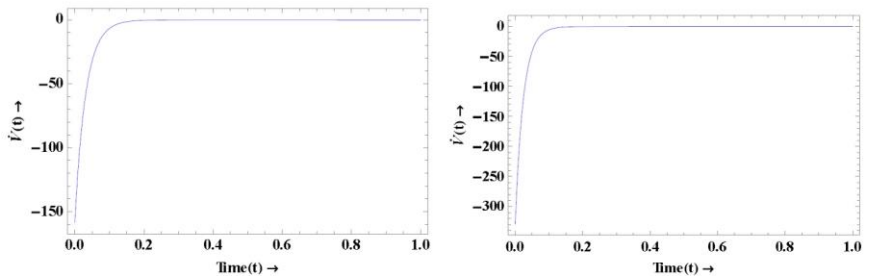


Figure 16

Time series graph of $\dot{V}(t)$ for the selected combination of the third order (a) in synchronization case (b) in anti-synchronization case.

In this subsection, the IMSS and IMSAS are formulated for the 7DHCS based on three error signals considered across all possible Leader-Follower pairings in which both the Leader-Follower subsystems consist of three state variables. Although a total of 20 such combinations exist (see Equation (12)),

only one representative case is analyzed; the remaining combinations can be examined following the same methodology. For the numerical investigation of the selected combination, the illustrative constants $k_{11} = 1$, $k_{12} = 1$, $k_{13} = 1$ were employed in the Mathematica-based simulations. The dynamical responses of the error systems and their associated state vectors for the combination under study are plotted to demonstrate the effectiveness of IMSS and IMSAS (see Figures 12–15). These figures clearly show that robust IMSS & IMSAS behavior is achieved. Furthermore, the time-series profile of $\dot{V}(t)$ (Figure 16) confirms that the combination under investigation attains the desired level of stability. For the third-order combination, the time required to reach satisfaction is slightly longer for IMSAS compared to IMSS.

4. Conclusions

This study introduces an active control-based approach to synchronize and anti-synchronize the various sub-dynamics of a hyperchaotic dynamical system internally. We identify three distinct types of heterogeneous combinations characterized by the errors and successfully demonstrate the implementation of IMSS AND IMSAS via the 7DCHS. Our computational work using Mathematica has validated the existence and achievement of IMSS and IMSAS for all presented heterogeneous type of combinations. However, a significant difference could not be observed between synchronization and anti-synchronization for all heterogeneous combinations under study though a minute delay in time response of stability could be seen in first and third order of combinations.

The proposed approach has several remarkable features, including the robustness and quick response time in the active control scheme with IMSS and IMSAS. Additionally, IMSS and IMSAS remove the external dependency from the follower system, allowing for internal division of the system into leader and follower systems as per the requirement. Furthermore, it provides someone a freedom to choose an appropriate order of combination as per the requirement.

Conflict of Interest

The authors declare that there is no conflict of interest.

References

[1] C. Anil Kumar, C. K. Narayanappa, S. Bhargavi, S. Harish, R. Krishna, K. R. Rekha, Varalakshmi, and S. Ashwini, "Nonlinear dynamics and chaos theory in engineering with applications in control systems and signal analysis," *J. Interdiscip. Math.*, vol. 28, no. 6, pp. 2099–2108 (2025), doi: 10.47974/JIM-2351.

[2] C. P. Selvan, A. Shrivastava, S. Ramaswamy, K. Shipra, A. Ashirova, K. Satone, and S. M. M. Naidu, "Applying control theory in engineering using dynamical systems methods," *J. Interdiscip. Math.*, vol. 29, no. 3, pp. 627–635 (2026), doi: 10.47974/JIM-2497.

[3] A. S. Al-Obeidi and S. F. Al-Azzawi, "Hybrid synchronization of high-dimensional chaos with self-excited attractors," *J. Interdiscip. Math.*, vol. 23, no. 8, pp. 1569–1584 (2020), doi: 10.1080/09720502.2020.1776941.

[4] S. Dhurve, T. Nanda, N. Kumari, and R. K. Upadhyay, "Chaos: Synchronization of two coupled GLV models using active and adaptive control techniques," *J. Dyn. Syst. Geom. Theor.*, vol. 19, no. 1, pp. 1–20 (2021), doi: 10.47974/JDSGT-2021-383.

[5] A. Malsaria, C. Joshi, S. Basu, and N. Sharma, "Secure chaotic cryptography for optical image encryption in pervasive devices using Lorenz-based DRPE, hybrid RSA-AES, and blockchain trust anchoring," *J. Discrete Math. Sci. Cryptogr.*, vol. 28, no. 8, pp. 3025–3037 (2025), doi: 10.47974/JDMSC-2464.

[6] H. Takhi, K. Kemih, L. Moysis, and C. Volos, "Passivity based sliding mode control and synchronization of a perturbed uncertain unified chaotic system," *Math. Comput. Simul.*, vol. 181, pp. 150–169 (2021), doi: 10.1016/j.matcom.2020.09.020.

[7] O. I. Olusola, K. S. Oyeleke, U. E. Vincent, and A. N. Njah, "Secure communication scheme based on synchronization of non-identical hyperchaotic systems," *J. Appl. Nonlinear Dyn.*, vol. 9, no. 2, pp. 273–285 (2020), doi: 10.5890/JAND.2020.06.009.

[8] K. Kemih, M. Halimi, M. Ghanes, H. Fanit, and H. Salit, "Control and synchronization of chaotic attitude control of satellite with backstepping controller," *Eur. Phys. J. Spec. Top.*, vol. 223, no. 8, pp. 1579–1589 (2014).

[9] Z. G. Wu, P. Shi, H. Su, and J. Chu, "Sampled-data fuzzy control of chaotic systems based on a T–S fuzzy model," *IEEE Trans. Fuzzy Syst.*, vol. 22, no. 1, pp. 153–163 (2013).

[10] A. Ucar, K. E. Lonngren, and E.W. Bai, "Multi-combinationing synchronization of chaotic systems with active controllers," *Chaos Solitons Fractals*, vol. 38, no. 1, pp. 254–262 (2008), doi: 10.1016/j.chaos.2006.11.041.

[11] X. Y. Wang and P. Sun, "Multi-combinationing synchronization of chaotic system with adaptive controllers and unknown parameters," *Nonlinear Dyn.*, vol. 63, pp. 599–609 (2011).

[12] J. Liu, J. Zhang, and Y. Wang, "Secure communication via chaotic synchronization based on reservoir computing," *IEEE Trans. Neural Netw. Learn. Syst.*, vol. 35, no. 1, pp. 285–299 (Jan. 2024), doi: 10.1109/TNNLS.2022.3173516.

[13] H. B. Zeng, K. L. Teo, Y. He, H. Xu, and W. Wang, "Sampled-data synchronization control for chaotic neural networks subject to actuator saturation," *Neurocomputing*, vol. 260, pp. 25–31 (2017).

[14] H. A. Abdullah, H. N. Abdullah, and W. A. Mahmoud Al-Jawher, "A hybrid chaotic map for communication security applications," *Int. J. Commun. Syst.*, vol. 33, no. 4, Art. no. e4236 (2020), doi: 10.1002/dac.4236.

[15] M. P. Aghababa and M. Saif, "Adaptive control realization for canonic Caputo fractional-order systems with actuator nonlinearity: application to mechatronic devices," *Adv. Differ. Equ.*, vol. 2020, no. 372 (2020), doi: 10.1186/s13662-020-02829-0.

[16] S. Vaidyanathan, A. Sambas, S. Kacar, and U. Cavusoglu, "A new finance chaotic system, its electronic circuit realization, passivity based synchronization and an application to voice encryption," *Nonlinear Eng.*, vol. 8, no. 1, pp. 193–205 (2019).

[17] A. Sambas, S. Vaidyanathan, S. Zhang, W. T. Putra, M. Mamat, and M. A. Mohamed, "Multistability in a novel chaotic system with perpendicular lines of equilibrium: analysis, adaptive synchronization and circuit design," *Eng. Lett.*, vol. 27, no. 4, pp. 744–751 (2019).

[18] A. Khan and S. Mittal, "Combination synchronization of time-delay chaotic system via robust adaptive sliding mode control," *Pramana*, vol. 88, no. 6, Art. no. 91 (2017), doi: 10.1007/s12043-017-1385-0.

[19] M. Shahzad, "Multi-combinationing synchronization of different orders: a generalization of increased/reduced order synchronization," *Iran J. Sci. Technol. Trans. Sci.*, vol. 44, no. 1, pp. 167–176 (2020).

[20] M. Shahzad, "General multi-switching synchronization using sliding mode control," *Eur. J. Control*, vol. 75, p. 100927 (2024), doi: 10.1016/j.ejcon.2023.100927.

[21] M. Shahzad, "Exploring the different order of switches during multi-switching synchronization," *Iranian J. Sci.*, vol. 48, no. 4, pp. 965–977 (2024), doi: 10.1007/s40995-024-01647-3.

[22] M. Shahzad, M. Raziuddin, and M. Naheed, "Internal synchronization using adaptive control," *Comput. Math. Methods,* vol. 2022, no. 1, Art. no. 2089151 (2022), doi: 10.1155/2022/2089151.

[23] M. Shahzad, "Internal synchronization using adaptive sliding mode," *Int. J. Robust Nonlinear Control*, vol. 33, no. 3, pp. 2320–2335 (2023), doi: 10.1002/rnc.6518.

[24] L. Runzi, W. Yinglan, and D. Shucheng, "Combination synchronization of three classic chaotic systems using active backstepping design," *Chaos*, vol. 21, no. 4, Art. no. 043114 (2011), doi: 10.1063/1.3655366.

[25] J. Z. Martinez, G. R. Gomez, and F. O. Espina, "A systematic approach for multi-switching compound synchronization of nonidentical chaotic systems using optimal control," in *Complex Systems and Their Applications. EDIESCA 2023*, E. Campos-Cantón, G. Huerta-Cuellar, E. Zambrano-Serrano, and E. Tlelo-Cuautle, Eds. Cham: Springer (2024), doi: 10.1007/978-3-031-51224-7_9.

[26] A. Khan, D. Khattar, and N. Agrawal, "Anti difference multiswitching compound–compound combination synchronization of seven chaotic systems," *Differ. Equ. Dyn. Syst.*, vol. 32, pp. 535–549 (2024), doi: 10.1007/s12591-021-00583-7.

[27] D. Liu, T. Li, and X. He, "Fixed-time multi-switch combined–combined synchronization of fractional-order chaotic systems with uncertainties and external disturbances," *Fractal Fract.*, vol. 7, no. 4, p. 281 (2023), doi: 10.3390/fractalfract7040281.

[28] M. Shahzad and I. Ahmad, "Experimental study of synchronization and anti-synchronization for spin orbit problem of Enceladus," *Int. J. Cont. Sci. Engin.*, vol. 3, no. 2, pp. 41–47 (2013).

[29] H. K. Zghair, S. A. Mehdi, and S. B. Sadkhan, "Design and analytic of a novel seven dimension hyper chaotic systems," in *2020 1st Information Technology to Enhance E-Learning and Other Application (IT-ELA)*, pp. 77–81 (2020), doi: 10.1109/IT-ELA50150.2020.9253077.

Received December, 2025